



24 **Abstract**

25 As photosynthetic producers, phytoplankton form the foundation of aquatic food webs.  
26 Understanding the relationships among photosynthetic traits in phytoplankton is essential to  
27 revealing how diversification of these traits allow phytoplankton to harvest energy from different  
28 light environments. We investigated whether the diversification of 15 species of cryptophytes, a  
29 phylum of phytoplankton with diverse light-capturing pigments, showed evidence of trade-offs  
30 among photosynthetic performance traits as predicted by the gleaner-opportunist resource  
31 exploitation framework. We constructed photosynthesis vs. irradiance (P-E) curves and rapid  
32 light curves (RLCs) to estimate parameters characterizing photosynthetic performance and  
33 electron transport rate. We inferred the evolutionary relationships among the 15 species with  
34 ultraconserved genomic elements and used a phylogenetically controlled approach to test for  
35 trade-offs. Contrary to our prediction, we observed a positive correlation between maximum  
36 photosynthetic rate,  $P_{max}$ , and  $P-E \alpha$ , an indicator of a species' sensitivity to increases in light  
37 intensity when light is a scarce resource. This result could not be explained by electron transfer  
38 traits, which were uncorrelated with photosynthetic rate. Together, our results suggest that  
39 ecological diversification of light exploitation in cryptophytes has escaped the constraints of a  
40 gleaner-opportunist tradeoff. Photosynthetic trade-offs may be context or scale dependent,  
41 thereby only emerging when investigated in situations different from the one used here.

42

43

44

45

46

47 **Introduction**

48        Trade-offs among traits can limit evolutionary diversification while simultaneously  
49        promoting ecological diversity (Buckling et al., 2003; Kneitel & Chase 2004; Blanchard &  
50        Moreau, 2016). Trade-offs constrain diversification by limiting the combinations of traits that are  
51        available to an organism, thereby restricting its ability to adapt to a novel environment.  
52        Conversely, trade-offs promote ecological diversity by preventing the emergence of a  
53        “Darwinian demon,” i.e., an organism that is optimally adapted to its environment in all respects  
54        and therefore outcompetes all other species in its community (Kneitel & Chase, 2004). Resource  
55        allocation trade-offs have been extensively studied because they are expected to strongly  
56        influence patterns of phenotypic variation. There has been less attention to trade-offs in resource  
57        acquisition and assimilation, however, even though these processes provide the foundation for  
58        allocation decisions and can confound predictions about allocation trade-offs (Van Noordwijk &  
59        de Jong, 1986). What work has been done has largely addressed consumers (Llandres et al.,  
60        2011), which potentially overlooks the importance of resource acquisition and assimilation trade-  
61        offs for primary producers.

62        The gleaner-opportunist trade-off describes a trade-off between maximum growth rate  
63        and minimum resource requirement,  $R^*$  (Grover, 1990; Bernhardt et al., 2020). A gleaner grows  
64        relatively well at low resource levels but relatively poorly at high resource levels (Figure 1a). In  
65        contrast, an opportunist grows relatively poorly at low resource levels but relatively well at high  
66        resource levels (Figure 1a). A gleaner, therefore, has a lower  $R^*$  value for the resource while an  
67        opportunist has a higher per-capita maximum growth rate. A lower  $R^*$  value indicates the ability  
68        for a population to persist at low levels of a resource, whereas a higher per-capita maximum  
69        growth rate indicates the ability to dominate a community when resources are abundant. Later,

70 the gleaner-opportunist framework was extended to include species-specific mortality rates  
71 (Litchman & Klaulsmeyer, 2001).

72 Gleaner-opportunist trade-offs are believed to be important in the maintenance of  
73 diversity in ecological communities (Litchman et al., 2007; Yamamichi & Letten, 2022). The  
74 underlying assumption is that this trade-off allows for the coexistence of multiple species when  
75 they are competing for a variable resource. Recent work, however, has called into question the  
76 existence and relative importance of the gleaner-opportunist trade-off in structuring communities  
77 (Kiørboe & Thomas, 2020; but see Letten & Yamamichi, 2021).

78 Here, we envision phytoplankton as consumers of light, and apply the gleaner-  
79 opportunist framework to the photosynthetic and physiological dynamics of light capture and  
80 exploitation. We take the view that evolutionary diversification is an important structuring force  
81 in ecological communities (McPeek, 1996). Thus, our aim is to test the predictions of this  
82 resource acquisition and assimilation framework as applied to the diversification of  
83 photosynthetic traits.

84

#### 85 *Phytoplankton and photosynthesis*

86 Phytoplankton form the foundation of most aquatic food webs (Field, 1998), thereby  
87 determining how much energy is available and influencing diversity at higher trophic levels.  
88 Phytoplankton show substantial variation of light capture and photosynthetic abilities. This  
89 includes variability of photosynthetic rates (Glover et al., 1987), of the wavelengths of light they  
90 can capture (Stomp et al., 2004), and of competitive abilities for light when light intensity  
91 fluctuates (Guislain et al., 2019). Light capture and subsequent photosynthetic performance can  
92 be considered key resource acquisition and assimilation traits (Richardson et al., 1983).

93 To investigate a potential gleaner-opportunist trade-off between photosynthetic traits, we  
94 performed a phylogenetically controlled analysis across a phylum of phytoplankton with diverse  
95 light capture abilities, the Cryptophyta. Cryptophytes are ideally suited to testing general  
96 predictions about photosynthetic trade-offs because they encompass substantial photosynthetic  
97 diversity, they are monophyletic, and they are commonly found in environments where  
98 competition for light may be strong. Cryptophytes' diverse light capture abilities stem from  
99 evolutionary diversification of their pigmentation (Doust et al., 2006; Greenwold et al., 2019).  
100 Cryptophyte light capture pigments include chlorophyll *a*, chlorophyll *c<sub>2</sub>*, and eight  
101 phycobiliproteins that are unique to cryptophytes (Hoef-Emden & Archibald, 2016). As a taxon,  
102 cryptophytes are defined as a monophyletic group by a unique secondary endosymbiosis event  
103 (Hoef-Emden & Archibald, 2016). Most other photosynthetic taxa have limited pigment  
104 diversity (if any at all), and analyses at higher taxonomic scales are complicated by reticulate  
105 evolution. Taken together, these characteristics of cryptophytes allow for comparative  
106 investigation of photosynthetic traits while controlling for shared evolutionary history.  
107 Furthermore, as frequent inhabitants of low-light environments, cryptophytes face strong  
108 pressure to optimize photosynthetic capabilities, making them a good model for investigating  
109 adaptive hypotheses about photosynthetic diversification. Other photosynthetic organisms that  
110 live in low-light environments such as shade-tolerant trees in northern hardwood forests (Walters  
111 & Reich, 1996), understory plants in forests (Craine & Dybzinski, 2013; Onoda et al., 2015), and  
112 coral symbionts (Anthony & Hoegh-Guldberg, 2003) lack either known pigment diversity or  
113 monophyly.

114 We estimated cryptophyte photosynthetic parameters using photosynthesis vs. irradiance  
115 curves (P-E curves; "E" is the standard symbol for irradiance in photophysiology; Kirk, 1994)

116 and rapid light curves (RLCs). P-E curves provide an estimate of an organism's maximum  
117 photosynthetic rate,  $P_{max}$ , when light is abundant, along with information about how rapidly rates  
118 of photosynthesis rise with increasing light intensity at low levels (Figure 1b). The initial slope  
119 of a P-E curve,  $\alpha$  (here referred to as  $P\text{-}E \alpha$ ), is the rate of photosynthesis per unit biomass per  
120 unit of incident light (Figure 1b).  $P\text{-}E \alpha$  measures how effectively an organism responds to light  
121 at sub-saturating intensities (Kirk, 1994).

122 RLCs provide information about photosynthesis on a short time scale and provide  
123 measurements of relative electron transport rate ( $rETR$ ), and effective quantum yield (Ralph &  
124 Gademann, 2005). Effective quantum yield is the proportion of absorbed photons that are used to  
125 drive electrons through photosystem II, whereas  $rETR$  is calculated by multiplying the quantum  
126 yield of photosynthesis by the photosynthetically active radiation. RLCs also provide estimates  
127 of the maximum relative electron transport rate,  $rETR_{max}$ , between photosystems II and I during  
128 the light-dependent reactions, and of the initial slope of a RLC (here referred to as  $RLC \alpha$ )  
129 (Ralph & Gademann, 2005).  $RLC \alpha$  is an estimate of the sensitivity of electron transfer to  
130 variation of light intensity at sub-saturating intensities (Ralph & Gademann, 2005) whereas  
131  $rETR_{max}$  is analogous to  $P_{max}$ ; it describes the maximum rate of electron transfer between  
132 photosystem II and photosystem I under saturating light. As electron transport underpins  
133 photosynthesis more broadly, measuring electron transport traits allows us to investigate  
134 mechanisms in more detail than P-E curves.

135

136 *Terminology and hypotheses*

137 One challenge for applying the gleaner-opportunist trade-off framework to  
138 photophysiology is that the use of photosynthetic traits and terminology may cloud any

139 discussion. For our study, maximum photosynthetic rate and maximum electron transport will  
140 take the place of maximum growth rate in the gleaner-opportunist framework. In the  
141 photosynthesis literature, prior authors have called  $P-E \alpha$  and  $RLC \alpha$  “efficiency” (Kirk, 1994;  
142 Ralph & Gademann, 2005), which may cause confusion with other uses in the literature on the  
143 ecology of resource exploitation (Watt, 1986; Raubenheimer & Simpson; 1996, Tessier et al.,  
144 2000). To avoid this confusion, we will use “sensitivity” to light intensity to refer to the  
145 biological interpretation of both  $P-E \alpha$  and  $RLC \alpha$ . Additionally, we have physiological rather  
146 than demographic data for our species, so we define a gleaner as one that performs better at low  
147 light levels but worse at high light levels (greater  $P-E \alpha/RLC \alpha$  but lower  $P_{max}/rETR_{max}$ )  
148 whereas an opportunist performs better at high light levels but worse at low light levels (lower  $P-$   
149  $E \alpha/RLC \alpha$  but higher  $P_{max}/rETR_{max}$ ,).

150 We hypothesized, that if a gleaner-opportunist trade-off exists, it would manifest as a  
151 negative linear relationship between  $P_{max}$  and  $P-E \alpha$ . Given that we found the opposite (see  
152 below), we hypothesized that this could be explained by a trade-off between the two parameters  
153 describing electron transport,  $rETR_{max}$  and  $RLC \alpha$ . Lastly, after examining both P-E curve and  
154 RLC data, we tested whether there was a positive relationship between photosynthetic rates and  
155 relative electron transport rates, predicting that greater electron transport would be correlated  
156 with a greater rate of carbon fixation.

157

## 158 **Methods**

### 159 *Culture conditions*

160 We used 15 species of cryptophytes in this experiment, 14 of which were obtained from  
161 culture repositories (Appendix S1: Section S1). We chose species to represent a wide range of

162 taxonomic, phylogenetic, and functional diversity. Each of the eight unique cryptophyte  
163 phycobilins are represented by at least one species in our dataset. We isolated one species from  
164 Congaree National Park, Congaree, SC, USA. Of the 15 species, 11 are identified to the species  
165 level, two to the genus level, while one, our new field isolate, is an undescribed species of  
166 *Cryptomonas* (Greenwold et al., unpublished data) Nine species are marine and six are  
167 freshwater. Additionally, we used *Goniomonas avonlea* (CCMP 3327), a non-photosynthetic  
168 cryptophyte, as an outgroup for phylogenetic estimation. More detailed culture information can  
169 be found in Appendix S1: Section S1.

170

171 *Photosynthesis vs. irradiance (P-E) curves*

172 A modified method of Lewis and Smith (1983) was used to measure photosynthesis as a  
173 function of irradiance (P-E). In short, NaH<sup>14</sup>CO<sub>3</sub> was added to a 20mL sample of each species,  
174 taken when cultures were growing at mid-exponential phase, to achieve a final activity of  
175 approximately 3  $\mu$ Ci mL<sup>-1</sup>. One mL of sample was then dispensed into each of 16 scintillation  
176 vials and vials were exposed to light intensities ranging from 0 -1400  $\mu$ mol photons m<sup>-2</sup> s<sup>-1</sup> and  
177 irradiance was measured with a quantum scalar irradiance sensor (Biospherical Instruments, Inc.,  
178 San Diego, CA, USA) inserted into an empty scintillation vial. Samples were incubated with <sup>14</sup>C  
179 for 20 minutes. After incubation, samples were terminated with 50  $\mu$ L buffered formalin while  
180 dissolved inorganic carbon was driven off by adding 200  $\mu$ L of 50% HCl and shaking the open  
181 vials for at least 12 h (usually overnight) in a fume hood. Five mL of scintillation cocktail  
182 (EcoLumeTM; MP Biomedicals, Solon, OH, USA) were then added to each vial, vials were  
183 mixed, and radioactive decay was counted using a Beckman LS-6500 scintillation counter  
184 (Beckman Coulter Inc., Brea, CA, USA). Photosynthetic rate for each species was measured

185 within a four-hour window (between 14:00 and 18:00 each day). Disintegrations per minute were  
186 then converted to chlorophyll *a*-specific primary productivity (Knap et al., 1996). Chlorophyll-  
187 specific rates of photosynthesis were plotted against light intensity and curves were fit with the  
188 equation of Platt et al. 1980 (Appendix S1: Equation S1).  $P_{max}$  and  $P-E \alpha$ , were calculated  
189 following Platt et al. 1980 (Appendix S1: Equation S2). More details about the P-E curve  
190 methods can be found in Appendix S1: Section S1.

191

192 *Rapid light curves and electron transport activity*

193 Parameters of electron transport for each species were assessed via the generation of  
194 RLCs using pulse-amplitude-modulated (PAM) chlorophyll *a* fluorescence with a Walz Water-  
195 PAM (PAM, Heinz-Walz, Germany). 20mL samples of each species, again taken at mid-  
196 exponential phase, were dark-adapted for 20 minutes and then 3mL sub-samples of each species  
197 were exposed to nine pulses of actinic light increasing in intensity with a range from 30 to 1300  
198  $\mu\text{mol photons m}^{-2}\text{s}^{-1}$  with a 30 second interval between each light pulse. Curves were fit like  
199 Equation S1, with  $P_S^B$  being replaced by  $rETR_{mPot}$  and  $P^B$  being replaced by  $rETR$  (Appendix S1:  
200 Equation S3). Estimates of  $rETR_{max}$  and  $RLC \alpha$  were calculated in the same manner as  $P_{max}$  and  
201  $P-E \alpha$  (Appendix S1: Equation S4). Electron transport traits were measured in triplicate for each  
202 species. More details about the RLC methods can be found in Appendix S1: Section S1.

203

204 *Phylogenetic estimation and comparisons across species*

205 Any relationships among photosynthetic traits in cryptophytes may be influenced by the  
206 species' shared evolutionary history, a problem that can be avoided with phylogenetic  
207 comparative approaches (Felsenstein, 1985). Therefore, we used phylogenetic generalized least

208 squares (PGLS) to control for phylogenetic history when testing for trade-offs (Martins &  
209 Hansen, 1997; Mundry, 2016). We first needed to reconstruct the evolutionary history of our  
210 species, which we did with ultraconserved elements (UCEs; Faircloth et al., 2012; 2015). This  
211 approach provides a genome-wide perspective on evolutionary relationships with thousands of  
212 loci, providing clear benefits over work with only one or two loci (Pamilo & Nei, 1988).

213 We extracted DNA from each of our species and sent DNA samples to RAPiD  
214 Genomics, LLC (Gainesville, Florida) where target enrichment sequencing was performed using  
215 Illumina 2 X 150 bp reads. We used RAxML version 8.0.19 for phylogenetic inference  
216 (Stamatakis, 2014) with sequence data from 1,868 conserved nuclear genome loci. Details of  
217 UCE probe design, DNA extraction and sequencing, and phylogenetic inference can be found in  
218 the supplementary material (Appendix S1: Section S1).

219

220 *Statistical analysis*

221 Photosynthetic and electron transport trait values were estimated with a non-linear least  
222 squares method using the *minpack.lm* package (Elzhov et al., 2016). We performed PGLS  
223 analyses in R version 3.6.2 (R Core Team, 2020) using the package *caper* (Orme et al., 2018).  
224 We tested for correlations between  $P_{max}$  and  $P-E \alpha$  and mean  $rETR_{max}$  and mean  $RLC \alpha$ . An  
225 analysis comparing  $P_{max}$  and  $rETR_{max}$  was also done post-hoc after examination of the P-E curve  
226 and RLC data. PGLS models were run with habitat, phycobiliprotein absorption peak, and cell  
227 volume as predictor variables. These were all non-significant predictors for all models  
228 (Appendix S1: Table S3), therefore all models are shown using only the single variable of  
229 interest as a predictor (Table 2). We used FigTree version 1.4.0  
230 (<https://github.com/rambaut/figtree/releases>) to produce the phylogenetic diagram (Figure 2),

231 rooting the phylogeny with *Goniomonas avonlea* (CCMP3327). All other figures were created  
232 using *ggplot2* (Wickham, 2016).

233

## 234 **Results**

### 235 *Photosynthetic parameter estimates*

236 Our estimates for  $P_{max}$  spanned two orders of magnitude, ranging from 0.071-7.10  $\mu\text{gC}$   
237  $\mu\text{Chl}^{-1} \text{h}^{-1}$ . Estimates for  $P-E \alpha$  almost spanned two orders of magnitude, ranging from 0.0035-  
238 0.11  $\mu\text{gC} \mu\text{Chl}^{-1} \text{h}^{-1}$  ( $\mu\text{mol photons m}^{-2} \text{s}^{-1}$ ) (Table 1). Variation of photosynthetic parameters  
239 estimated from the RLCs were constrained to less than one order of magnitude, ranging from  
240 16.96-89.66  $\mu\text{mol electrons m}^{-2} \text{s}^{-1}$  for  $rETR_{max}$  and 0.19-0.37  $\mu\text{mol electrons photons}^{-1}$  for  $RLC \alpha$   
241 (Table 1). We also compared our estimates to photosynthetic parameter values estimated by the  
242 Marine Primary Production: Model Parameters from Space (MAPPS) project, which contains  
243 estimates of photosynthetic parameters from a global set of 5,711 P-E experiments with marine  
244 phytoplankton (Bouman et al., 2018). Our estimates for  $P_{max}$  and  $P-E \alpha$  for the 15 species of  
245 cryptophytes used in this study are in the typical range of estimates from the MAPPS project,  
246 indicating that cryptophytes do not have extreme photosynthetic traits (Appendix S1: Section S2,  
247 Figure S2).

248

### 249 *Cryptophyte phylogeny*

250 We inferred a phylogeny (Figure 2) with two main clades: 1) a *Hemiselmis/Chroomonas*  
251 clade, and 2) a *Cryptomonas/Rhodomonas* clade. All nodes were strongly supported. To our  
252 knowledge, the phylogeny presented here is the first to apply a broad genome-wide data set to  
253 Cryptophyta.

254 *Tests of trade-offs between photosynthetic traits*

255  $P_{max}$  and  $P-E \alpha$  are positively correlated (Figure 3a, Table 2) with the correlation having a  
256 negligible phylogenetic signal (Table 2). We found no evidence of a correlation between the  
257 maximum relative electron transport rate,  $rETR_{max}$  of a species and the initial slope of its RLC,  
258  $RLC \alpha$  (Figure 3b, Table 2). There was, however, a strong phylogenetic signal (Table 2). We did  
259 not find evidence of a correlation between  $P_{max}$  and  $rETR_{max}$  (Figure 3c, Table 2) however a  
260 phylogenetic signal was detected (Table 2).

261

## 262 **Discussion**

263 *No evidence of a gleaner-opportunist trade-off*

264 We investigated whether diversification of cryptophyte algae shows a trade-off between  
265 photosynthetic traits in the context of a gleaner-opportunist framework. We accounted for  
266 evolutionary history in our analyses, allowing us to exclude evolutionary history as a driver of  
267 the presence or absence of correlations among traits.

268 We found no evidence of a gleaner-opportunist trade-off between photosynthetic  
269 performance traits in cryptophytes. In fact, we found the opposite: a significant positive  
270 correlation between  $P_{max}$  and  $P-E \alpha$  (Figure 3a). Cryptophytes that respond better to variation of  
271 light at low levels also perform better at high light levels, suggesting that photosynthesis is  
272 optimized simultaneously across a broad range of light intensities. All species were exposed to  
273 light intensities that ranged from 0 -1400  $\mu\text{mol photons m}^{-2} \text{s}^{-1}$ , which reflect light intensity levels  
274 that marine and freshwater algae encounter in natural environments (Kirk, 1994). The intensities  
275 on the higher end of this range are sufficient to induce photoinhibition in many algae, which is  
276 when  $P_{max}$  begins to decrease as light intensity increases (Kirk, 1994). The P-E curves for our

277 species, however, do not show evidence of photoinhibition (Appendix S2). Cryptophytes are  
278 usually described as low light specialists (Gervais, 1997; Hoef-Emden & Archibald, 2016) but  
279 our data suggest that at least some cryptophytes photosynthesize relatively well at high light  
280 levels.

281 Photosynthetic rate often correlates with population growth rate (Falkowski et al., 1985;  
282 Coles & Jones, 2000) and is argued to represent the relative fitness of photosynthetic organisms  
283 (Violle et al., 2007). Therefore, species with the largest values for  $P-E \alpha$  and  $P_{max}$  are expected to  
284 have higher average fitness in across a wide range of light intensities, compared against species  
285 with lower trait values.

286 Prior work has shown that the relationship between maximum growth rate and the initial  
287 slope of a functional response is strongly positively correlated with body size (Kiørboe &  
288 Thomas, 2020). We accounted for this potential allometric relationship by including cell volume  
289 as a fixed effect in our PGLS models and did not see a significant correlation between it and the  
290 initial slope of a P-E curve or RLC. (Appendix S1: Table S3). Therefore, differences of cells'  
291 volumes cannot explain the observed lack of a gleaner-opportunist trade-off.

292 There have been disagreements in the literature as to the relative importance, and even  
293 existence, of the gleaner-opportunist trade-off (Kiørboe & Thomas, 2020). It has long been  
294 assumed to play a crucial role in structuring ecological communities by allowing for coexistence  
295 between unequal competitors. We took a novel approach to evaluate the potential origin of this  
296 type of trade-off through evolutionary diversification of the traits themselves by using  
297 phylogenetic comparative methods to control for the evolutionary history of our focal species. As  
298 we did not find a gleaner-opportunist trade-off between photosynthetic traits our work supports

299 the view that this trade-off may not be as widespread as previously assumed (Litchman et al.,  
300 2007; Isanta-Navarro et al., 2022; Yamamichi & Letten, 2022).

301 There are, however, caveats to our results. One is that we did not incorporate species-  
302 specific mortality rates into our experiment. With the inclusion of mortality rates, an opportunist  
303 is defined by the ratio of its maximum growth rate to its mortality rate rather than simply being  
304 the species with the higher maximum growth rate when a resource is abundant (Litchman &  
305 Klausmeier, 2001). The trade-off could then potentially emerge between a species with a low  
306 resource requirement and one with a high ratio of maximum growth rate to mortality rate  
307 (Litchman & Klausmeier, 2001). In the context of our study, the ratio for defining an opportunist  
308 would be the ratio of maximum photosynthetic rate to mortality rate. By ignoring mortality rates  
309 we are potentially overlooking a condition through which a gleaner-opportunist trade-off may  
310 manifest.

311

312 *No evidence of electron transport trade-offs*

313 A possible explanation for the lack of a trade-off at the scale of overall photosynthesis is  
314 that an assimilation trade-off may exist in the electron transport chain of the light reactions but is  
315 masked by compensation in other parts of photosynthesis. This explanation is however excluded  
316 by our electron transport rate data, which showed no relationship between the initial slope of a  
317 species' RLC and its maximum relative electron transport rate (Figure 3b).

318 The positive relationship between  $P-E \alpha$  and  $P_{max}$  could have arisen due to a mechanistic  
319 link between photosynthesis and electron transport. We expected species that were transferring  
320 more electrons between photosystems II and I to show a higher maximum photosynthetic rate as  
321 a higher rate of electron transport which would allow for more carbon to be fixed during the

322 Calvin Cycle (Falkowski & Raven, 2007). We tested whether maximum photosynthetic rate was  
323 positively correlated with maximum rate of electron transfer. Somewhat surprisingly, we found  
324 no evidence of a relationship (Figure 3c), indicating that greater electron transport between  
325 photosystems does not yield greater photosynthesis. This relationship, however, would really be  
326 expected only if all the energy generated by electron transport is being used to fix carbon.  
327 Physiological plasticity in diverting energy generated through electron transport to alternative  
328 metabolic pathways may explain the absence of this correlation (Halsey & Jones, 2015).

329

330 *An escape from photosynthetic trade-offs?*

331 Trade-offs promote ecological diversity by allowing competing species to coexist.  
332 Competitors may experience trade-offs in resource acquisition, resource allocation, differential  
333 predation, or dispersal ability; all these mechanisms can create the conditions necessary for  
334 stable coexistence (Chesson, 2000; Chase & Leibold, 2003; Ellner et al., 2019). Our data shows  
335 no evidence for a gleaner-opportunist trade-off between photosynthetic traits in cryptophytes.  
336 Thus, some cryptophytes should be strong competitors across a wide range of light  
337 environments. This lack of a trade-off, specifically between  $P_{max}$  and  $P-E \alpha$ , has been observed  
338 before and physiological mechanisms have been suggested as the cause of this relationship  
339 (Behrenfeld et al., 2008; Halsey et al., 2010).

340 In ecological comparisons of phytoplankton growing in different nutrient environments,  
341 Halsey et al. (2011; 2013; 2014) suggested positive covariation between  $P_{max}$  and  $P-E \alpha$  is driven  
342 by carbon metabolism occurring via different pathways. These researchers manipulated nitrogen  
343 or light to limit growth rates in green algae and diatoms, thereby producing positive covariation  
344 of  $P_{max}$  and  $P-E \alpha$  across environments due to changes in carbon metabolism. They argue that at

345 low growth rates, induced by nitrogen or light limitation, a fixed transient carbon pool is quickly  
346 used for synthesis of ATP or NADPH, nucleic acids, and lipids. In contrast, at high growth rates  
347 fixed transient carbon is mostly stored as polysaccharides and used over a longer timescale.  
348 Thus, these within-species environmental manipulations recovered the same pattern as our  
349 across-species evaluation of evolutionary diversification, but it is unclear whether the proposed  
350 mechanism could be the same. First, in our study, all cultures were grown in nutrient-rich media  
351 for short periods of time, and thus none should have been nitrogen-limited. This is particularly  
352 true because our measurements were taken at mid-exponential phase. Second, we do not have  
353 information on the transient carbon pool or polysaccharide storage to characterize carbon  
354 metabolism in cryptophytes. Knowing a positive relationship exists, acquiring these types of data  
355 becomes a priority for future work.

356 The carbon metabolism hypothesis provides a potential explanation for the observed lack  
357 of gleaner-opportunist and power-efficiency trade-offs but does not rule out the possibility that  
358 trade-offs occur between other resource acquisition traits that we did not investigate. In fact, its  
359 empirical link to nitrogen limitation points to the importance of considering different types of  
360 resources. Trade-offs among resource acquisition traits in phytoplankton are well known, such as  
361 being a strong competitor for light but a weak competitor for nutrients (Tilman, 1977; Litchman  
362 & Klausmeier, 2008). Phytoplankton resource acquisition traits are remarkably plastic (Stomp et  
363 al., 2008; Hattich et al., 2016) so environmental variability such as intermittent predation  
364 pressure, sporadic nutrient limitation, interspecific competition, or temperature shifts could  
365 potentially drive the emergence of photosynthetic trade-offs. Over evolutionary timescales,  
366 cryptophytes that display low trait values for both  $P_{max}$  and  $P-E \alpha$  may have optimized other

367 aspects of fitness to be excellent competitors for other resources, leading to trade-offs among  
368 traits not investigated in this study.

369

370 *Implications for natural phytoplankton communities*

371 While our study aimed to broadly examine photosynthetic trade-offs through the gleaner-  
372 opportunist framework, our results also imply that the niches of cryptophytes in natural  
373 phytoplankton communities may be misunderstood. In particular, the realized niche of  
374 cryptophytes may have historically been interpreted as their fundamental niche. Cryptophytes are  
375 often described as low-light specialists (Hoef-Emden & Archibald, 2016) and frequently occur at  
376 deeper depths where less light is available (Gervais, 1997). At these depths, light attenuation  
377 leads to a decrease in the number of photons available for photosynthesis and alters the color of  
378 available light. Absorption by chlorophyll *a* and colored dissolved organic matter reduces the  
379 blue light present in the environment while green and red light are absorbed by accessory  
380 pigments like phycoerythrin and phycocyanin. In conjunction with the MAPPS data (Appendix  
381 S1: Figure S2), our results suggest that cryptophytes are not exceptional at capturing photons at  
382 low light intensities when compared to other taxa of phytoplankton, in contrast to expectations  
383 for low-light specialists. Furthermore, our P-E curves (Appendix S2) provide no evidence for  
384 photoinhibition at high light intensities. Cryptophytes instead have a broad fundamental niche  
385 with respect to light intensity and are better thought of as low-light tolerant rather than  
386 specialists. Cryptophytes may use their unique pigmentation to absorb colors of light that are not  
387 absorbed by taxa present at the surface. They could be exploiting fine gradations of light color  
388 rather than light intensity to carve out realized niches in different aquatic ecosystems. In addition  
389 to being able to exploit different colors of light, cryptophytes may succeed at deeper depths

390 because due to greater nutrient availability than surface waters. Cryptophytes require nitrogen for  
391 phycobiliprotein synthesis (Doust et al., 2006) and have been shown to rapidly degrade these  
392 nitrogen-containing pigments when nitrogen is scarce (Da Silva et al., 2009). Living deeper may  
393 provide cryptophytes with access to sufficient nitrogen to synthesize phycobiliproteins, which  
394 then allows them to exploit wavelengths of light for photosynthesis that are not absorbed by  
395 other taxa.

396

397 *Future directions for trade-off research*

398 Trade-offs may be dependent on the scale at which they are investigated (i.e., at the level  
399 of phenotype, genotype, population, or species) (Agrawal, 2020). For example, a relationship  
400 may be seen from a within-species comparison, but the same relationship may not manifest at the  
401 among-species level. This pattern of trade-offs occurring across different scales can be seen in  
402 trade-offs between milkweed leaf traits (Agrawal, 2020). A trade-off between leaf mass per area  
403 and cardenolide concentration can be seen between populations but is not apparent at the level of  
404 genotype or species (Agrawal, 2020). For plant traits, the general expectation is that trade-offs or  
405 predicted trade-offs will not be persistent across different scales (Agrawal, 2020). This paradigm  
406 of scale-dependent trade-offs may also be applicable to phytoplankton and may provide an  
407 investigative framework for future work on photosynthetic trait trade-offs.

408 Our study tested for photosynthetic trade-offs within an explicit resource exploitation  
409 framework while controlling for evolutionary history via phylogenetic comparative methods.  
410 This approach should be applicable for researchers working in systems where competition for  
411 light among photosynthetic organisms plays a strong role in structuring communities. This may  
412 include aquatic macrophytes (Sand-Jensen et al., 2007), forest communities (Onoda et al., 2015),

413 grassland communities (Dybinski & Tilman, 2007; Hautier et al., 2009), and coral  
414 endosymbionts (McIlroy et al., 2019). Examining strategies for light capture through pre-existing  
415 ecological frameworks can provide new perspectives and insights on how photosynthetic  
416 organisms interact with light in their environment.

417

#### 418 **Acknowledgments**

419 We thank Kristin Heidenreich, Krista Harmon, Cameron Riddick, and Patrick Lawson for  
420 help with culture maintenance and Jay Pinckney for the inspiration and equipment for measuring  
421 electron transport rate via rapid light curves. This study was supported by the National Science  
422 Foundation (NSF) Dimensions of Biodiversity program under grant #1542555 to T.L.  
423 Richardson and J. L. Dudycha.

424

#### 425 **Author Contributions**

426 The experiment was designed by JAS, TLR, and JLD. Data for the P-E curves and RLCs  
427 were collected by JAS. DNA extractions and phylogeny creation was done by MJG. Statistical  
428 analyses were done by JAS. The manuscript was written by JAS, MJG, and JLD with all authors  
429 contributing to the editing process.

430

#### 431 **Conflicts of Interest**

432 The authors declare no conflicts of interest.

433 **References**

434 Anthony, K.R.N., and O. Hoegh-Guldberg. 2003. "Variation in Coral Photosynthesis,  
435 Respiration and Growth Characteristics in Contrasting Light Microhabitats: An Analogue  
436 to Plants in Forest Gaps and Understoreys?". *Functional Ecology* 17: 246-259.

437 Behrenfeld, M.J., K.H. Halsey, and A.J. Milligan. 2008. "Evolved Physiological Responses  
438 of Phytoplankton to their Integrated Growth Environment". *Philosophical Transactions  
439 of the Royal Society B* 363: 2687-2703.

440 Bernhardt, J.R., P. Kratina, A.L., Pereira, M. Tamminen, M.K., Thomas, and A. Narwani  
441 2020. "The Evolution of Competitive Ability for Essential Resources". *Philosophical  
442 Transactions of the Royal Society B* 375: 20190247.

443 Blanchard, B. D., and C.S. Moreau. 2017. "Defensive Traits Exhibit an Evolutionary Trade-Off  
444 and Drive Diversification in Ants". *Evolution* 71: 315–328.

445 Bouman, H. A., T. Platt, M. Doblin, F.G. Figueiras, K. Gudmundsson, H.G. Gudfinnsson, B.  
446 Huang, et al. 2018. "Photosynthesis–Irradiance Parameters of Marine Phytoplankton:  
447 Synthesis of a Global Data Set". *Earth System Science Data* 10: 251–266.

448 Buckling, A. 2003. "Adaptation Limits Diversification of Experimental Bacterial Populations".  
449 *Science* 302: 2107–2109.

450 Chase, J. M., and M.A. Leibold. 2003. *Ecological Niches: Linking Classical and Contemporary  
451 Approaches*. Chicago, IL: University of Chicago Press.

452 Chesson, P. 2000. "Mechanisms of Maintenance of Species Diversity". *Annual Review of  
453 Ecology and Systematics* 31: 43-366.

454 Craine, J.M., and R. Dybzinski. 2013. "Mechanisms of Plant Competition for Nutrients, Water,  
455 and Light". *Functional Ecology* 27: 833-840.

456 Doust, A. B., K.E. Wilk, P.M.G. Curmi, and G.D. Scholes. 2006. "The Photophysics of  
457 Cryptophyte Light-Harvesting". *Journal of Photochemistry and Photobiology, A* 184: 1–  
458 17.

459 Dybzinski, R., and D. Tilman. 2007. "Resource Use Patterns Predict Long-Term Outcomes of  
460 Plant Competition for Nutrients and Light". *The American Naturalist* 170: 305-318.

461 Ellner, S. P., R.E. Snyder, P.B Adler, and G. Hooker. 2019. "An Expanded Modern Coexistence  
462 Theory for Empirical Applications". *Ecology Letters* 22: 3-18.

463 Elzhov, T.V, K.M, Mullen, A.N. Speiss, and B. Bolker. 2016. "minpack.lm: R Interface to the  
464 Levenberg-Marquardt Nonlinear Least-Squares Algorithm Found in MINPACK, Plus  
465 Support for Bounds. R package version 1.2-1".  
466 <https://CRAN.Rproject.org/package=minpack.lm>

467 Faircloth, B. C., M.G. Branstetter, N.D. White, and S.G. Brady. 2015. "Target Enrichment of  
468 Ultraconserved Elements from Arthropods Provides a Genomic Perspective on  
469 Relationships among Hymenoptera". *Molecular Ecology Resources* 15: 489-501.

470 Faircloth B.C., J.E. McCormack, N.G Crawford, M.G. Harvey, R.T. Brumfield, and T.C. Glenn.  
471 2012. "Ultraconserved Elements Anchor Thousands of Genetic Markers Spanning  
472 Multiple Evolutionary Timescales". *Systematic Biology* 61: 717-726.

473 Felsenstein, J. 1985. "Phylogenies and the Comparative Method". *The American Naturalist* 125:  
474 1–15.

475 Field, C. B. 1998. "Primary Production of the Biosphere: Integrating Terrestrial and Oceanic  
476 Components". *Science* 281: 237–240.

477 Gervais, F. 1997. "Light-Dependent Growth, Dark Survival, and Glucose Uptake by  
478 Cryptophytes Isolated from a Freshwater Chemocline". *Journal of Phycology* 33: 18–25.

479 Glover, H. E., M.D. Keller, and R.W. Spinrad. 1987. "The Effects of Light Quality and Intensity  
480 on Photosynthesis and Growth of Marine Eukaryotic and Prokaryotic Phytoplankton  
481 Clones". *Journal of Experimental Marine Biology and Ecology* 105: 137–159.

482 Greenwold, M. J., B.R. Cunningham, E.M. Lachenmyer, J.M. Pullman, T.L. Richardson, and J.L.  
483 Dudycha. 2019. "Diversification of Light Capture Ability was Accompanied by the  
484 Evolution of Phycobiliproteins in Cryptophyte Algae". *Proceedings of the Royal Society  
485 B* 286: 20190655.

486 Grover, J. P. 1990. "Resource Competition in a Variable Environment: Phytoplankton Growing  
487 According to Monod's Model". *The American Naturalist* 136: 771–789.

488 Guislain, A., B.E. Beisner, and J. Köhler. 2019. "Variation in Species Light Acquisition Traits  
489 Under Fluctuating Light Regimes: Implications for Non-Equilibrium Coexistence". *Oikos*  
490 128: 716–728.

491 Halsey, K. H., and B.M. Jones. 2015. "Phytoplankton Strategies for Photosynthetic Energy  
492 Allocation". *Annual Review of Marine Science* 7: 265–297.

493 Halsey, K.H., A.J. Milligan, and M.J. Behrenfeld. 2010. "Physiological Optimization Underlies  
494 Growth Rate-Independent Chlorophyll-Specific Gross and Net Primary Production".  
495 *Photosynthesis Research* 103: 125–137.

496 Halsey, K.H., A.J. Milligan, and M.J. Behrenfeld. 2011. "Linking Time-Dependent Carbon-  
497 Fixation Efficiencies in *Dunaliella Tertiolecta* (Chlorophyceae) to Underlying Metabolic  
498 Pathways". *Journal of Phycology* 47: 66-76.

499 Halsey, K.H., R.T. O'Malley, J.R. Graff, A.J. Milligan, and M.J. Behrenfeld. 2013. "A Common  
500 Partitioning Strategy for Photosynthetic Products in Evolutionarily Distinct  
501 Phytoplankton Species". *New Phytologist* 198: 1030-1038.

502 Hattich, G. S. I., L. Listmann, J. Raab, D. Ozod-Seradj, T.B.H. Reusch, and B. Matthiessen.

503 2017. "Inter- and Intraspecific Phenotypic Plasticity of Three Phytoplankton Species in

504 Response to Ocean Acidification". *Biology Letters* 13: 20160774.

505 Hautier, Y., P.A. Niklaus, and A. Hector. 2009. "Competition for Light Causes Plant

506 Biodiversity Loss After Eutrophication". *Science* 324: 636-638.

507 Hoef-Emden, K., and J.M. Archibald. 2016. "Cryptophyta (Cryptomonads)". In *Handbook of the*

508 *Protists*, edited by J.M. Archibald, A.G.B. Simpson, C.H. Slamovits, L. Margulis, M.

509 Melkonian, D.J. Chapman, and J.O. Corliss, 1-41. Springer International Publishing.

510 Isanta-Navarro, J., T. Klauschies, A. Wacker, and D. Martin-Creuzburg. 2022. "A Sterol-

511 Mediated Gleaner–Opportunist Trade-Off Underlies the Evolution of Grazer Resistance

512 to Cyanobacteria". *Proceedings of the Royal Society B* 289: 20220178.

513 Kiørboe, T., and M.K. Thomas. 2020. "Heterotrophic Eukaryotes Show a Slow-Fast Continuum,

514 Not a Gleaner–Exploiter Trade-Off". *Proceedings of the National Academy of Sciences*

515 117: 24893-24899.

516 Kirk, J. T. O. 1994. *Light & Photosynthesis in Aquatic Ecosystems*. Cambridge, UK: Cambridge

517 University Press.

518 Knap, A., A. Michaels, A. Close, H.W. Ducklow, and H. Dickson. 1996. "Protocols for the Joint

519 Global Ocean Flux Study (JGOFS) Core Measurements. Report no. 19, Reprint from

520 the IOC Manuals and Guides no. 29". Bergen: UNESCO.

521 Kneitel, J. M., and J.M. Chase. 2004. "Trade-Offs in Community Ecology: Linking Spatial

522 Scales and Species Coexistence". *Ecology Letters* 7: 69–80.

523 Letten, A.D., and M. Yamamichi. 2021. "Gleaning, Fast and Slow: In Defense of a Canonical  
524 Ecological Trade-Off". *Proceedings of the National Academy of Sciences*, 118:  
525 e2022754118.

526 Lewis, M., and J. Smith. 1983. "A Small Volume, Short-Incubation-Time Method for  
527 Measurement of Photosynthesis as a Function of Incident Irradiance". *Marine Ecology  
528 Progress Series* 13: 99–102.

529 Litchman, E., and C.A. Klausmeier. 2001. "Competition of Phytoplankton Under Fluctuating  
530 Light". *The American Naturalist* 157: 170–187.

531 Litchman, E., C.A. Klausmeier, O.M. Schofield, and P.G. Falkowski. 2007. "The Role of  
532 Functional Traits and Trade-Offs in Structuring Phytoplankton Communities: Scaling  
533 from Cellular to Ecosystem Level". *Ecology Letters* 10: 1170-1181.

534 Llandres, A. L., E. De Mas, and M.A. Rodríguez-Gironés. 2012. "Response of Pollinators to the  
535 Tradeoff between Resource Acquisition and Predator Avoidance". *Oikos* 121: 687–696.

536 Martins, E.P., and T.F. Hansen. 1997. "A General Approach to Incorporating Phylogenetic  
537 Information into the Analysis of Interspecific Data". *The American Naturalist* 149: 646–  
538 667.

539 McIlroy, S.E., R. Cunning, A.C. Baker, and M.A. Coffroth. 2019. "Competition and Succession  
540 Among Coral Endosymbionts". *Ecology and Evolution* 9: 12767-12778.

541 McPeek, M. A. 1996. "Linking Local Species Interactions to Rates of Speciation in  
542 Communities". *Ecology* 77: 1355-1366.

543 Mundry, R. 2014. "Statistical Issues and Assumptions of Phylogenetic Generalized Least  
544 Squares". In *Modern Phylogenetic Comparative Methods and their Application in*

545           *Evolutionary Biology*, edited by L.Z. Garamszegi, 131-153. Springer-Verlag Berlin  
546           Heidelberg.

547   van Noordwijk, A. J., and G. de Jong. 1986. "Acquisition and Allocation of Resources: Their  
548           Influence on Variation in Life History Tactics". *The American Naturalist* 128: 137–142.

549   Onoda, Y., J.B. Saluñga, K. Akutsu, S. Aiba, T. Yahara., and N.P.R. Anten. 2014. "Trade-off  
550           between Light Interception Efficiency and Light Use Efficiency: Implications for Species  
551           Coexistence in One-Sided Light Competition". *Journal of Ecology* 102: 167-175.

552   Orme, D., R. Freckleton, G. Thomas, T. Petzoldt, S. Fritz, N. Isaac, and W. Pearse. 2018.  
553           "caper: Comparative Analyses of Phylogenetics and Evolution in R. R Package Version  
554           1.0.1". <https://CRAN.R-project.org/package=caper>

555   Pamilo, P., and M. Nei. 1988. "Relationships between Gene Trees and Species Trees". *Molecular  
556           Biology and Evolution* 5: 568-583.

557   Platt, T., C.L. Gallegos, and W.G. Harrison. 1980. "Photoinhibition of Photosynthesis in Natural  
558           Assemblage of Marine Phytoplankton". *Journal of Marine Research* 38: 687-701.

559   Ralph, P. J., and R. Gademann. 2005. Rapid Light Curves: A Powerful Tool to Assess  
560           Photosynthetic Activity. *Aquatic Botany* 82: 222–237.

561   Raubenheimer, D., and S.J. Simpson. 1996. "Meeting Nutrient Requirements: The Roles of  
562           Power and Efficiency". *Entomologia Experimentalis et Applicata*, 80, 65–68.

563   Richardson, K., J. Beardall, and J.A. Raven. 1983. Adaptation of Unicellular Algae to Irradiance:  
564           an Analysis of Strategies. *New Phytologist* 93: 157–191.

565   R Core Team 2020. R: A Language and Environment for Statistical Computing. R  
566           Foundation for Statistical Computing, Vienna, Austria. <https://www.R-project.org/>.

567   Sand-Jensen, K., T. Binzer, and A.L. Middelboe. 2007. "Scaling of Photosynthetic Production of

568                    Aquatic Macrophytes – A Review". *Oikos* 116: 280-294.

569                    da Silva, A. F., S.O. Lourenço, and R.M. Chaloub. 2009. Effects of Nitrogen Starvation on the  
570                    Photosynthetic Physiology of a Tropical Marine Microalga *Rhodomonas* sp.  
571                    (Cryptophyceae). *Aquatic Botany* 91: 291–297.

572                    Stamatakis, A. 2014. "RAxML version 8: a tool for phylogenetic analysis and post-analysis of  
573                    large phylogenies". *Bioinformatics* 30: 1312-1313.

574                    Stomp, M., M.A. van Dijk, H.M.J. van Overzee, M.T. Wortel, C.A.M. Sigon, M. Egas, H.  
575                    Hoogveld, H.J. Gons, and J. Huisman. 2008. "The Timescale of Phenotypic Plasticity and  
576                    its Impact on Competition in Fluctuating Environments". *The American Naturalist* 172:  
577                    E169–E185.

578                    Stomp, M., J. Huisman, D. Gerla, M. Rijkeboer, B.W. Ibelings, U.I.A. Wollenzien, and L.J. Stal.  
579                    2004. "Adaptive Divergence in Pigment Composition Promotes Phytoplankton  
580                    Biodiversity". *Nature* 432: 104-107.

581                    Tessier, A. J., M.A. Leibold, and J. Tsao. 2000. "A Fundamental Trade-Off in Resource  
582                    Exploitation by *Daphnia* and Consequences to Plankton Communities". *Ecology* 81:  
583                    826–841.

584                    Tilman, D. 1977. "Resource Competition between Plankton Algae: An Experimental and  
585                    Theoretical Approach". *Ecology* 58: 338–348.

586                    Violette, C., M.L. Navas, D. Vile, E. Kazakou, C. Fortunel, I. Hummel, and E. Garnier. 2007. "Let  
587                    the Concept of Trait Be Functional!" *Oikos* 116: 882–892.

588                    Walters, M.B., and P.B. Reich. 1996. "Are Shade Tolerance, Survival, and Growth Linked? Low  
589                    Light and Nitrogen Effects on Hardwood Seedlings". *Ecology* 77: 841-853.

590 Watt, W. B. 1986. "Power and Efficiency as Indexes of Fitness in Metabolic Organization". *The*  
591 *American Naturalist* 127: 629–653.

592 Wickham, H. 2016. "ggplot2: elegant graphics for data analysis". Springer-Verlag New  
593 York.

594 Yamamichi, M., and A.D. Letten. 2021. "Rapid Evolution Promotes Fluctuation-Dependent  
595 Species Coexistence". *Ecology Letters* 24: 812-818.

596 Yamamichi, M., and A.D. Letten. 2022. "Extending the Gleaner-Opportunist Trade-Off".  
597 *Journal of Animal Ecology* 00:1-8.

598

599

600

601

602

603

604

605

606

607

608

609

610 **Table 1:** Values for photosynthetic performance traits and electron transport rate traits for each  
 611 cryptophyte species

Species	$P-E \alpha$ ( $\mu\text{gC} \mu\text{Chl} \text{a}^{-1} \text{h}^{-1}$ ( $\mu\text{mol}$ photons $\text{m}^{-2} \text{s}^{-1}$ ) $^{-1}$ )	$P_{max}$ ( $\mu\text{gC} \mu\text{Chl} \text{a}^{-1} \text{h}^{-1}$ )	$RLC \alpha$ ( $\mu\text{mol}$ electrons photons $^{-1}$ )	$rETR_{max}$ ( $\mu\text{mol electrons}$ $\text{m}^{-2} \text{s}^{-1}$ )
<i>Cryptomonas ovata</i>	0.030	3.07	0.323	58.86
<i>Chroomonas mesostigmatica</i>	0.065	2.84	0.205	21.28
<i>Chroomonas nordstedtii</i>	0.0035	0.072	0.297	35.86
<i>Chroomonas placoidea</i>	0.023	2.67	0.194	21.83
<i>Chroomonas sp.</i>	0.015	0.24	0.222	20.78
<i>Cryptomonas sp.</i>	0.048	1.93	-	-
<i>Guillardia theta</i>	0.024	3.19	0.301	67.06
<i>Hemiselmis cryptochromatica</i>	0.11	2.66	0.256	27.06
<i>Hemiselmis pacifica</i>	0.031	1.79	0.356	16.96
<i>Hemiselmis tepida</i>	0.030	1.43	0.212	19.04
<i>Proteomonas sulcata</i>	0.058	3.05	0.367	29.31
<i>Rhodomonas minuta</i>	0.061	3.47	0.323	89.66
<i>Rhodomonas salina</i>	0.018	1.56	0.374	30.29
<i>Teleaulax sp.</i>	0.039	2.24	0.374	77.74
<i>Unid. sp.</i>	0.10	7.10	0.328	35.89

612

613

614

615

616

617 **Table 2:** Summary of results from PGLS regression models. Significant  $p$ -values are in bold.

618

619

PGLS Model	Intercept	$F$	Df	Adjusted $R^2$	$p$	N	Pagel's $\lambda$
$P_{\max} \sim P\text{-}E\text{-}\alpha$	0.88	12.12	1,13	0.44	<b>0.0041</b>	15	0.054
$r\text{ETR}_{\max} \sim$ $\text{RLC}\text{-}\alpha$	20.66	0.53	1,12	-0.038	0.48	14	1
$P_{\max} \sim r\text{ETR}_{\max}$	2.64	0.038	1,12	-0.080	0.85	14	1

620

621

622

623

624

625

626

627

628

629

630

631

632

633

634

635

636

637

638

639

640

641 **Figure 1:** a) Visualization of the gleaner-opportunist framework, adapted from Litchman &  
642 Klausmeier, 2001. A gleaner (blue line) has a higher per-capita growth rate at low resource  
643 concentrations while an opportunist (gold line) has a higher per-capita growth when resources  
644 are abundant. b) Example photosynthesis vs. irradiance curve for the cryptophyte *Rhodomonas*  
645 *salina* indicating the initial slope of the P-E curve,  $P\text{-}E \alpha$ , and the maximum photosynthetic rate,  
646  $P_{max}$

647

648 **Figure 2:** Phylogeny for the 15 cryptophyte species constructed using ultra-conserved elements.  
649 Bootstrap values shown at each node.

650

651 **Figure 3:** Relationships between photosynthetic parameters derived from P-E curves and RLC.  
652 a) Maximum photosynthetic rate,  $P_{max}$  ( $\mu\text{g C} (\mu\text{ chl } a)^{-1} \text{ h}^{-1}$ ), of a species and  $P\text{-}E \alpha$  ( $\mu\text{g C} (\mu\text{ chl } a)^{-1} \text{ h}^{-1} (\mu\text{mol photons m}^{-2} \text{ s}^{-1})^{-1}$ ), the initial slope of its P-E curve. b) Maximum relative electron  
653 transport rate,  $rETR_{max}$  ( $\mu\text{mol electrons m}^{-2} \text{ s}^{-1}$ ) and the initial slope of a RLC,  $RLC \alpha$  (electrons  
654 photons $^{-1}$ ). Points are the mean values of triplicate estimates for  $rETR_{max}$  and  $RLC \alpha$  for each  
655 species or species. c) No correlation between the maximum photosynthetic rate of a species,  $P_{max}$   
656 ( $\mu\text{g C} (\mu\text{ chl } a)^{-1} \text{ h}^{-1}$ ), and its maximum relative electron transport rate,  $rETR_{max}$  ( $\mu\text{mol electrons}$   
657  $\text{m}^{-2} \text{ s}^{-1}$ ).  $rETR_{max}$  values represent the mean of triplicate estimates for each species or species.

659

660

661

662

663

664

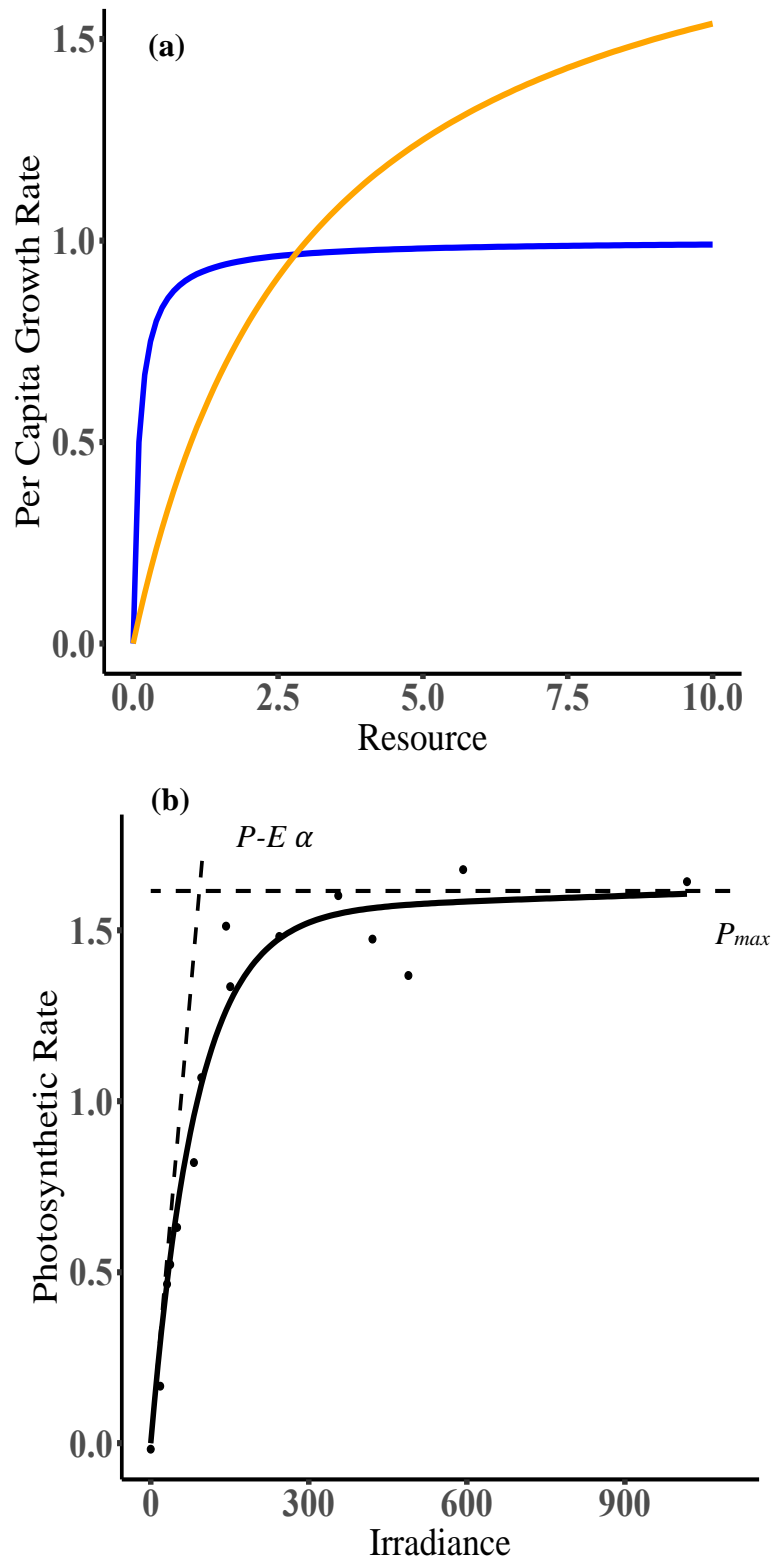
665

666

667

668

669 **Figure 1**  
670



715 **Figure 2**

716

717

718

719

720

721

722

723

724

725

726

727

728

729

730

731

732

733

734

735

736

737

738

739

740

741

742

743

744

745

746

747

748

749

750

751

752

753

754

755

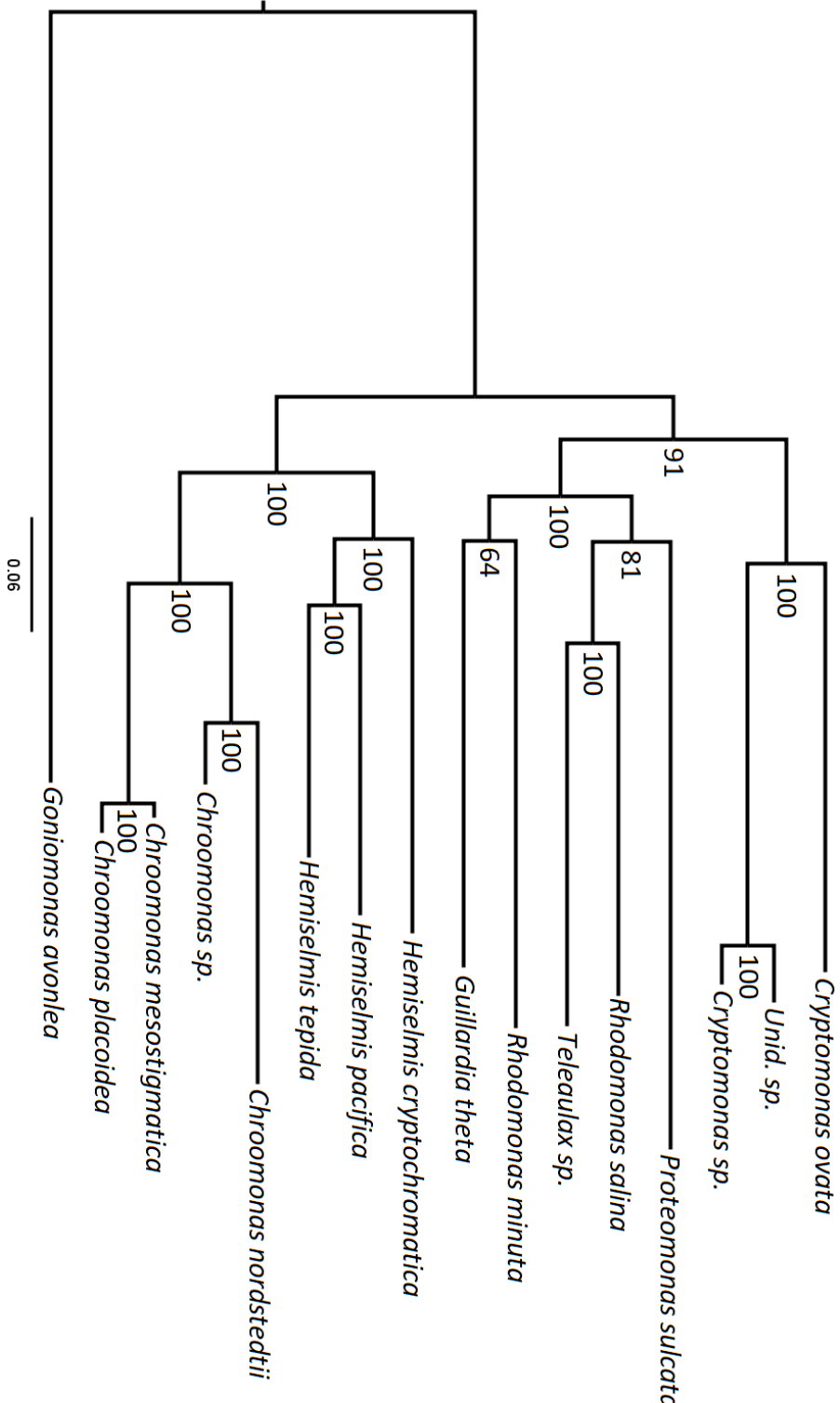
756

757

758

759

760



761  
762  
763  
764  
765  
766  
767  
768  
769  
770  
771  
772  
773  
774  
775  
776  
777  
778  
779  
780  
781  
782  
783  
784  
785  
786  
787  
788  
789  
790  
791  
792  
793  
794  
795  
796  
797  
798  
799  
800  
801  
802  
803  
804  
805  
806

**Figure 3**

